

A Small Satellite Preliminary Thermal Control and Heat Shield Analysis

by

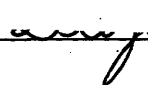
Diego A. Melani Barreiro

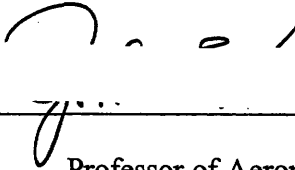
SUBMITTED TO THE DEPARTMENT OF MECHANICAL ENGINEERING IN
PARTIAL FULFILLMENT OF THE REQUIREMENTS FOR THE DEGREE OF

BACHELOR OF SCIENCE
AT THE
MASSACHUSETTS INSTITUTE OF TECHNOLOGY

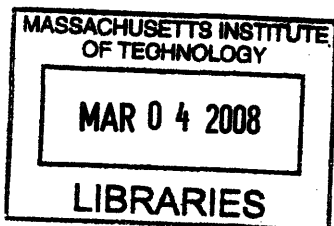
FEBRUARY 2008

© 2006 Massachusetts Institute of Technology
All rights reserved

Signature of Author:  _____
Department of Mechanical Engineering
December 13, 2006

Certified by:  _____
John E. Keesee
Professor of Aeronautics and Astronautics
Thesis Supervisor

Accepted by:  _____
John H. Lienhard V
Professor of Mechanical Engineering
Chairman, Undergraduate Thesis Committee



ARCHIVES

A Small Satellite Preliminary Thermal Control and Heat Shield Analysis

by

Diego A. Melani Barreiro

Submitted to the Department of Mechanical Engineering
on December 13, 2006 in Partial Fulfillment of the Requirements
for the Degree of Bachelor of Science in
Mechanical Engineering

ABSTRACT

As part of a student owned small satellite project, a preliminary thermal control and heat shield analysis was developed to verify acceptable performance requirements for the system. For the thermal control section, the analysis was focused on the Bus module of the satellite. It measured the effects of the Sun and Eclipse periods at low earth orbit (LEO), accounted key design and subsystems interaction considerations and indicated some of the structural parameters available for its success. As for the heat shield section, calculations were made to quantify the magnitude of the heat flux going into the payload capsule.

The thermal control analysis was implemented to determine if the radiator area and insulation from the aluminum honeycomb structure were sufficient to maintain the electronic components at proper operating temperatures during the mission. Materials such as insulating coating paints and mechanisms such as heaters were researched and considered as additional thermal protection barriers. Thermal subsystems interfaces, i.e. Bus-Return Vehicle Interface, were also analyzed.

Models for the incoming heat across the Ablator heat shield were used to determine values for transient and steady-state heating and cooling scenarios. These provided indications of the incoming and outgoing heat transfers into and out of the payload module. With the use of thermal resistance models, values for the heat transfers were obtained.

This study interpreted the thermal effects of orbiting Earth at LEO for the Bus module of a small satellite. It also measured the effectiveness of the heat shield on preventing incoming heat transfers into the payload module. From proper approximations, realistic results were obtained for both cases. Though no in depth analysis was performed, actual values obtained for the heating effects provided a valid scope of the overall effects on the system.

Thesis Supervisor: John E. Keesee
Title: Professor of Aeronautics and Astronautics

CONTENT

1.1	Thermal Control	5
1.1.1	Derived Level 3 Requirements	5
1.1.2	Thermal Control Design.....	6
1.1.2.1	Satellite Bus Thermal Considerations	6
1.1.2.2	Payload and EDLS Thermal Considerations	8
1.1.2.3	Materials & Mechanisms	8
1.1.2.4	Heaters and Sensors.....	9
1.1.3	Thermal Subsystem Interfaces.....	10
1.1.3.1	Structures	10
1.1.3.2	Bus/RV Interface	11
1.2	Heat Shield Analysis	12
1.2.1	METHOD	13
1.2.1.1	Cylinder Model.....	14
1.2.1.2	Flat Plate Model.....	15
1.2.2	RESULTS	16
1.2.2.1	Steady State	16
1.2.2.2	Transient.....	18
1.2.3	CONCLUSION.....	22
2	REFERENCES	23
3	APPENDIX A: EQUATIONS AND METHODS.....	24
4	APPENDIX B: GRAPHS , DATA OBTAINED and CAD MODELS	32

TABLES AND FIGURES

Table 1. Derived Thermal Control Requirements.....	6
Table 2. Black Paints	9
Table 3. BUS Radiator Area.....	10
Table 4. Analysis Parameters	14
Table 5. Steady State Heat Up Period Results	17
Table 6. Steady State Cool Down Period Results.....	18
Table 7. External Heat Input Comparison	33
Figure 1 Overall System Heat Interactions	5
Figure 2 Temperature Lines vs. Dissipated Heat.....	11
Figure 3. Satellite's Position around Earth	12
Figure 4. Heat Shield Profile (Dimensions in mm)	13
Figure 5. Payload Module Side View (Dimensions in cm)	14
Figure 6. Cylindrical Model (a) versus Flat Plate Model (b).	15
Figure 7. Steady State Thermal Circuit	16
Figure 8. Two Node Panel Model.....	19
Figure 9. Heat Up 1 st Orbit	20
Figure 10. Heat Up 2 nd Orbit	21
Figure 11. Side Panels Incoming Heat.....	32
Figure 12. Temperature versus radiator area	33
Figure 13. Bus Dimension in millimeters.....	34
Figure 14. Payload/Heat Shield Dimensions in centimeters	35

1.1 Thermal Control

The Thermal control subsystem is responsible for maintaining operating temperatures for satellite components, as well as transferring and radiating heat from the Payload and EDLS¹ systems. During the thermal control design process, emphasis was placed on simplicity and reliability.

The control system should be able to manage the different interactions within the system and its exterior. This is briefly summarize in the following figure.

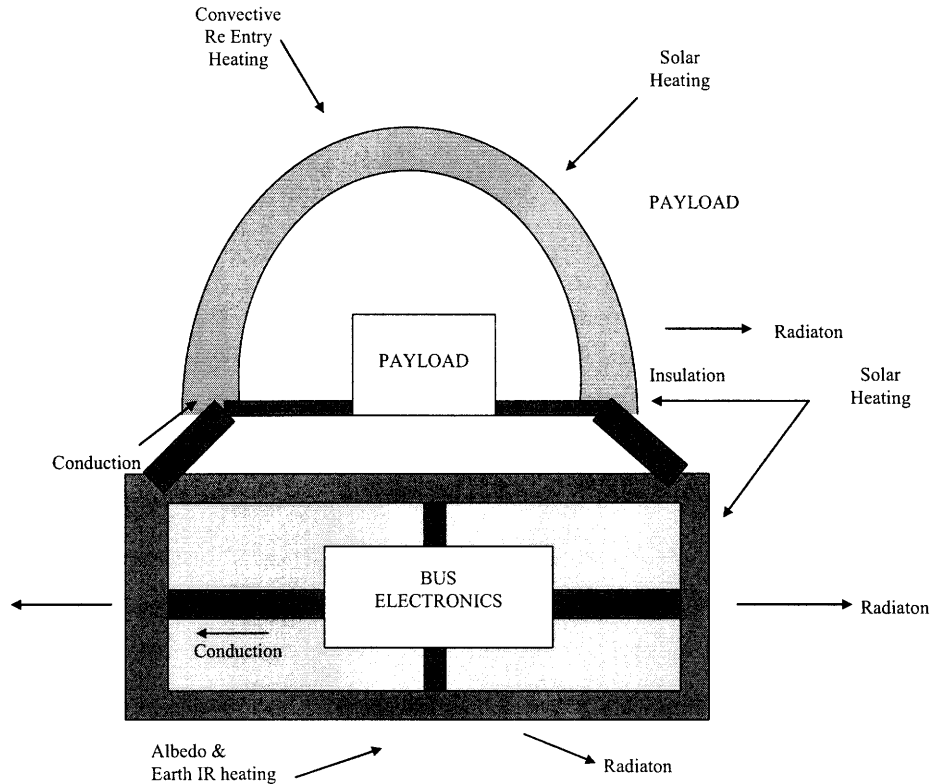


Figure 1. Overall System Heat Interactions

The Thermal Control design is preliminary, and no detailed nodal analyses have been computed. Preliminary models indicate that this control system will function according to requirements.

1.1.1 Derived Level 3 Requirements

¹ EDLS stands for Entry Descent and Landing System

Table 1. Derived Thermal Control Requirements²

Number	Requirement	Parent	Rationale
thm-01	The s/c shall maintain adequate temperatures for s/c components	msn-04, pro-05, pro-07	Satellite components will have varying temperature operating ranges
thm-02	The cost to build the thermal system shall be less than \$TBD (FY2010 dollars).	bus-13	This is the budget allocated to the development of the thermal controls system.
thm-03	The thermal system shall be ready for installation by date TBD.	bus-14	In order to meet schedule deadlines, the thermal system must be completed by this date.
thm-04	The mass of thermal system shall be less than TBD kg including contingency.	bus-15	This is the mass allocated to the thermal system.
thm-05	The system shall provide for the rejection or storage of 450 W ³ of heat from the bus	msn-04, pro-05, pro-07	Avoid slow build up of heat
thm-06	The system shall provide for the removal of dissipated heat from temperature sensitive components	msn-04, pro-05, pro-07	Avoid creating hot spots that cause component temperature to get too high
thm-07	The system shall provide for any heat produced by heaters inside the Bus module	msn-04, pro-05, pro-07	Avoid getting too cold

1.1.2 Thermal Control Design

In order to provide the satellite with the proper thermal control to ensure the mission's success, certain aspects should be observed. These should cover the thermal considerations for the infrastructure and components during the various periods of the mission as well as the elements used to provide protection and insulation.

1.1.2.1 Satellite Bus Thermal Considerations

The primary concern of the thermal subsystem for the satellite bus is maintaining operating temperatures for the hydrazine tanks/lines and electrical components. To maintain such temperatures (generally ranging from -30°C to 40°C for the electrical components, with the exception of the propellant, which may require heating since has a smaller allowable temperature range), the thermal system utilizes passive heat radiation from the satellite base plate and side panels. Electrical components combined with resistive heaters (along with insulation added, where necessary) keep the temperature above its minimum bound, while heat radiation from the side plate (to which all electrical

² Some of this parameters are still being determined.

³ Preliminary estimate of the heat produce by the electronics and the amount of heat coming from the payload. More information can be found in the Appendix section.

components are mounted) insures that the systems equilibrium temperature is less than the maximum temperature bound. Additionally, radiators can be painted with different colored paints, effectively changing their emissivity and solar absorptivity to allow further control over equilibrium temperatures.

Maximum values for incoming Sun, Albedo and Earth IR effects have been calculated along with the radiator's performance to account for the heat dissipation⁴. The results of these are mentioned in the following sections.

1.1.2.1.1 SATELLITE'S SUN PERIOD

During this period the Module will be exposed to incoming sun at the top face, and Albedo and Earth IR effects at the bottom. The top area of the bus is about $.1526 \text{ m}^2$ ⁵, where the bottom area is 1.08 m^2 . The max solar heat coming at the top of the bus equals 36.8 W . The bottom receives 80.5 W from the Albedo effects and 41.9 W from the Earth IR. Due to the position of the satellite, there will be Albedo and Earth IR effects on the side panels during this period as well. With the assumption that these are directly effective on the surface, i.e. perpendicular to the face that is being affected, the max value for the Albedo becomes 115 W and for the Earth IR 60 W . This was also modeled as if the side panels were just a panel of the total size of the 8 side panels. (Area of each side panel: $.347 \text{ m}^2$ for a Total Side Panel Area of 2.776 m^2 .) Since the satellite will be rotating, the heating effect will be uniformly distributed over the 8 side panels. This is why the approximation of the modeling serves as a worst case scenario since it considers the total area of the 8 side panels.

1.1.2.1.2 SATELLITE'S ECLIPSE PERIOD

During this period the Module will be exposed to just incoming Earth IR to the top face and side panels. These values are 32.1 W for the top and 137.1 W ⁶ for the side panels.

The main concern during this period is the BUS bottom since there is no incoming heat of any sort and thus it will be exposed to the low temperature of the space environment ($\sim 3 \text{ K}$). Currently, there is just the Aluminum Alloy 7075 T6 to account for any thermal protection, and this is not enough. Considerations should focus on insulating the bottom plate to help protect the batteries and propulsion tanks, since they will be placed on this area, from the cold temperature. This will also help minimize the period for which the heaters will need to be on and thus reducing the duration of the power requirement.

1.1.2.1.3 ELECTRICAL COMPONENTS LOCATION AND MOUNTING

Electronics will be placed inside boxes and mounted on the side panels. Proper passive systems should be considered in order to properly dissipate the heat out to the radiators and not into the BUS. Insulation can be provided on the sides that are not facing the

⁴ Refer to Appendix A for calculations

⁵ Please refer to figures 13 and 14 in Appendix B

side panel in order to conduct the heat in that direction. The heat is trying to escape this insulation will provide a path for it to exit. If the heat dissipation is too large in comparison to the area of the actual component and sink plate, fins can be used to conduct the heat uniformly from the radiators.

1.1.2.2 Payload and EDLS Thermal Considerations

As the heat shield and MLI surrounding the Payload are an excellent insulator, heat dissipated within the Payload and EDLS systems must be transferred to the Satellite Bus for radiation. Again, as within the Satellite's Bus, equilibrium temperatures compatible with the temperature tolerances of the mice will be achieved by a combination of resistive heaters and heat conduction and radiation, which will transfer the heat into the bus compartment.

Heat generated within the Payload and EDLS systems will be conducted from those locations by structural supports/trusses to the structural interface with the Satellite Bus. At this interface, the separation system encourages conduction across the interface by providing an increased cross-sectional area that is directly in contact with the EDLS system. This component in turn conducts heat to the side panels and base plate, which then radiates the heat. As with the side plate radiation, the base plate can be painted with different color paints to modify its absorptivity and infrared emissivity; thereby, modifying its equilibrium temperature

1.1.2.3 Materials & Mechanisms

As mentioned earlier, several tools are used to control temperatures within different portions of the satellite.

1.1.2.3.1 MULTI LAYER INSULATION (MLI)

MLI is a blanket type insulation consisting of several separated sheets of Mylar or Kapton and is widely used in the satellite industry for its excellent insulation and low mass and volume. MLI only works in a vacuum. Because of this, MLI is being considered mainly for components in the bus, which may be in danger of getting too cold. In particular, the propellant tanks, which have especially high lower temperature boundaries, are at risk.

1.1.2.3.2 Z-93 WHITE PAINT

Since the purpose of spacecraft radiators is to dump waste heat to space, it is desirable for them to have a high infrared emissivity and low solar absorptivity so as to dump waste heat at a faster rate while taking in as little as possible of the solar heat input. To this end, it was decided by the University of Washington to use Z-93 white paint, which has an emissivity $\epsilon = 0.9$ and a solar absorptivity $\alpha_s = 0.15$. Z-93 white paint has also flown on previous satellites, and was less expensive than many other white paints investigated by UW. The current cost of this paint is around \$177 per pint and each one

⁶ See appendix A Section II

covers as much as 10 ft². For our purposes we may need to use up to 6 pints; putting the cost of paint around \$1062⁷.

1.1.2.3.3 CHEMGLAZE Z304 BLACK PAINT

In order to improve heat transfer from the RV interface and electronics deck to the radiators, it was decided to paint internal components with high emissivity paint. Chemglaze Z304 black paint was chosen by UW because it has an emissivity of $\epsilon = 0.9$, it has been used in space, and it is relatively inexpensive. Current prices for black paints with similar thermal properties fluctuate between \$700 and \$1000 per pint⁸.

Table 2. Black Paints

Paint	Cost/pint
MLS-85SB Silicon Black	\$ 717
RM550IB Inorganic	\$ 1016

1.1.2.4 Heaters and Sensors

As it pertains to the BUS Module, heaters may be necessary for, at least, the propulsion system components. It is possible that they will also be needed for other components but this decision will come as further analysis is performed. Tentatively there is a good candidate in MINCO for supplying us with the heaters. They sell Kapton patch heaters that are space approved and tested. They are also suggested by the GSPC⁹ as a good option for spacecraft applications. Their power requirement will depend on factors such as the duration of heating the elements as well as the area to be heated. As there is not a final decision on the choice of the propulsion system to be used, only an approximation of the needed power can be given. Just to give an example of the performance of these heaters, a 3" by 6" heater will have an effective area of heating of 15.74 in².

As for temperature sensors, thermocouples offer the option of indicating temperature changes without requiring any power input. They are two different metals wires joined at one end. When a temperature change is observed, it causes a change in the electromotive force (emf) and thus increasing the output voltage.

While thermocouples are a good option, there is also the possibility of using thermistors and RTD (Resistance Temperature Detectors). The RTD is a metallic device that, due to changes in temperature, shows a resistance change. In the case of the thermistors, the change in resistance is recorded from a ceramic semiconductor and not a metal like the RTD.

The advantages of thermistors and RTD is that they offer a more stable and accurate reading; however, thermocouples offer a wider range of reading temperatures. Also there is a limitation from the thermistors, due to the fact that they are resistive devices,

⁷ AZ Technology Estimates

⁸ AZ Technology Estimates

⁹ Goddard Space Flight Center Qualified Parts List Directory

and a heat production is associated with them which can affect their overall performance.

In order to operate the heaters and sensors, thermal switches should be added to the overall thermal interface. This will required some power, again, depending on what heating system is then developed. Honeywell is a potential provider of the thermal switches

1.1.3 Thermal Subsystem Interfaces

The thermal control subsystem interfaces with many areas including Payload, EDLS, and other subsystems in the bus including structures, power, propulsion and navigational components. The control system interface with the Payload and EDLS will monitor temperatures and dissipate or add heat as needed to keep all the systems within their operational temperature ranges. The structural interfaces include the placements of any sensors and heaters, and also the sizing of structural members needed to conduct or radiated heat. The interfaces within the other subsystems should take into account the different operational temperatures of the component as well as the need for insulation and heaters throughout the mission duration.

1.1.3.1 Structures

The specific placements of the thermocouples and ohmic heaters are not yet known. Additionally the size of the structural supports may need to be increased for improved conduction rates since the structural panels and members act as thermal conduits and radiators.

1.1.3.1.1 RADIATORS

Radiators can be place at three locations in the BUS: Top Face, Side Panels and the Bottom Face. Table 3 shows the locations with their respective radiator's area.

Currently the faces are to be made out of an Aluminum 7075-T6 Alloy Honeycomb. This type of material offers a core thermal conductivity ranging from 1W/m-K (lighter core) to 5 W/m-K (heavier core). The dissipation of heat under this honeycomb settings could present an issue with the overall temperature of the inside of the BUS module since preliminary conduction analysis showed that the inside face was about the same as the outside, thus as same as the radiator side. It will get cold inside and proper insulation should be included.

Table 3. BUS Radiator Area¹⁰

Location	Possible Radiator Area [m ²]
TOP	.1526
BOTTOM	1.08
SIDE PANELS	1.5438
TOTAL:	2.776

¹⁰ Please refer to figures 12 in Appendix B

The radiator's performance is going to depend on its outside temperature.¹¹ The higher the temperature of the outside face of the radiator, the better. Including the external heat inputs, the payload's input of 70 W and a estimated 150 W¹² from the electronics, for the maximum area of 2.776 m² the BUS can dissipate the total heat (~ 450 W) at a temperature no lower than 236 K (-37.15 C). This means that if the outside temperature of the radiators is below this mark, it will be unable to dissipate that amount of heat. Figure 1 below shows how this compares to other temperatures and heat inputs. If the max load changes from 450 W, it will still be possible to read the new optimal temperature from just looking at the graph.

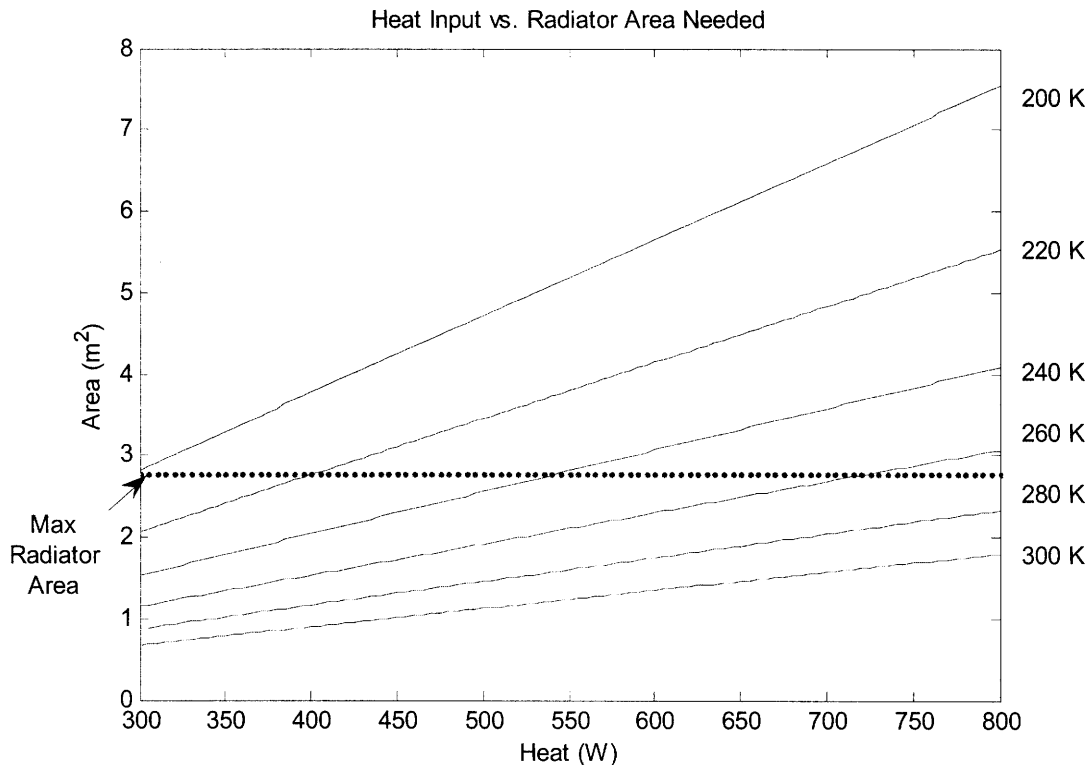


Figure 2 Temperature Lines vs. Dissipated Heat

1.1.3.2 Bus/RV Interface

The thermal loads to be transferred across the interface are significant and pose a threat to the sensitive electronic devices and wiring immediately surrounding the BUS/RV interface. Because of this, an adequate duct for the passage of thermal energy must be integrated as part of the BUS/RV interface itself. UW considered the use of the Planetary Systems Lightband; this had a thermal conductivity of 121.11W/m-K.

¹¹See Appendix A Part III

¹² Estimation similar to Karam's estimation .

The new separation system being considered is from the Space Vector Corporation. It is made out of Aluminum 7075-T6 and it has a thermal conductivity of 130 W/m-K. The temperature at the RV side of the separation system is that the same of the Payload which is 288.15 K (15 C). We also know that the new estimated heat transfer is 70 W from the Payload to the BUS, thus a conduction analysis gives a minimal variation in the temperature of the BUS which is 287.547 K (14.424 C)¹³

1.2 Heat Shield Analysis

Due to the recent uncertainties about the performance of the heat shield in supplying sufficient protection to the payload module, an approximate but accurate thermal analysis was carried out. Concerns about the possibility of heat going through the heat shield into the mice environment as well as the heat going out during the eclipse phase suggested the analysis.

This analysis, despite simplistic, presents a view of the actual external energy incidence effect that was not considered before. Throughout the duration of the mission, the Mars Gravity Biosatellite will be exposed to both sun and Earth IR effects during the Sun and Eclipse face respectively. Figure 1 below presents an overview picture of the satellite's location with respect to the Earth and the Sun.

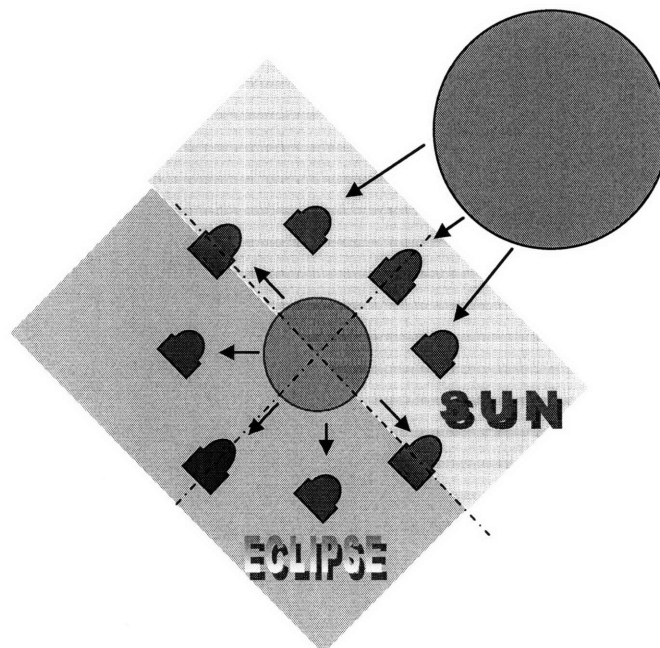


Figure 3. Satellite's Position around Earth

The heat shield to be used for the satellite is provided by Applied Research Associates, Inc. We will be using an SRAM-20 Ablator with a thickness variance from around 7 mm to 25 mm along the curved path of it. This Ablator material has a very low

¹³ See appendix A section III

thermal conductivity, thus providing with a very small heat flux across it. This amount of heat flux is what we sought from the analysis. The following sections will present the development of the analysis and the thought process behind it.

1.2.1 METHOD

The approach here taken was to model the payload bucket as simply as possible, taking the assumptions necessary to deliver a sound but straightforward analysis. Different approaches were taken at the time of performing the analysis in order to obtain the closest approximation, these are further explained below. For the upcoming indications it will be good to provide certain figures and tables indicating some of the measurements taken. Let's begin with a profile look of the heat shield as shown in figure 3 and an overall payload capsule drawing in figure 4.

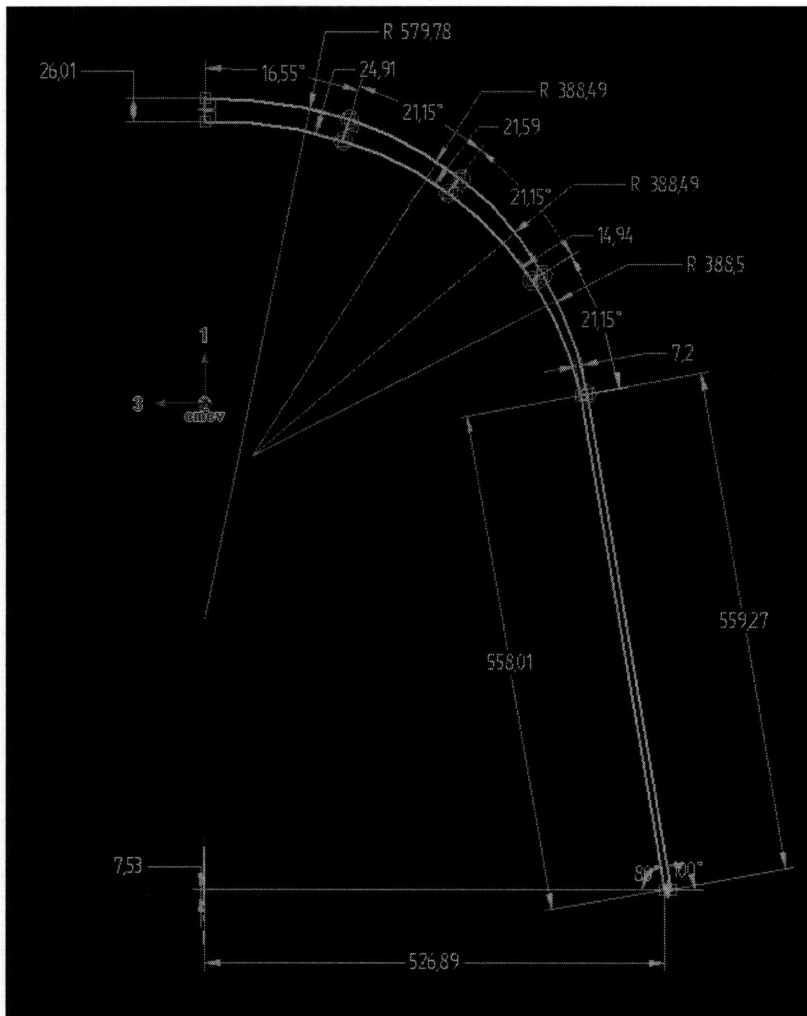


Figure 4. Heat Shield Profile (Dimensions in mm)

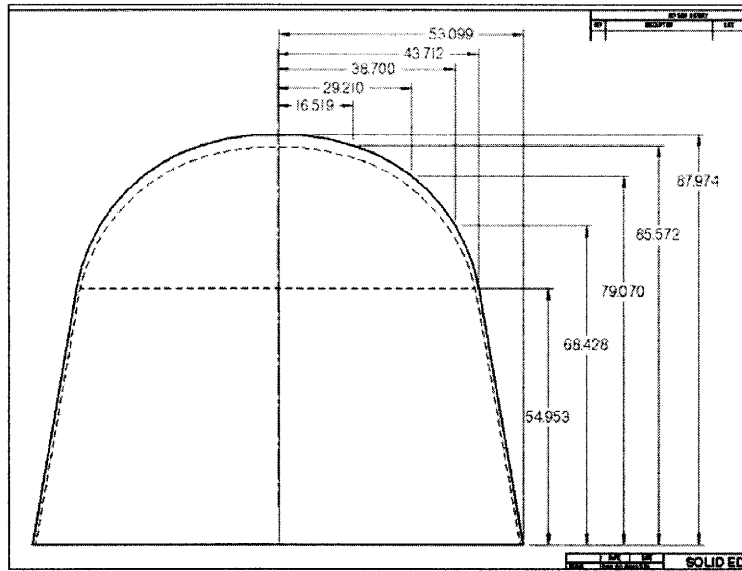


Figure 5. Payload Module Side View (Dimensions in cm)

The following table provides some reference values for areas and dimensions that will be regularly referred to in the analysis.

Table 4. Analysis Parameters

PARAMETER	VALUE
Inner Radius of Sphere	.43012 meters
Outer Radius of Sphere	.43712 meters
Height of Cylinder	.87974 meters
Heat Shield Thickness	.007 meters
MLI Thickness	0.055 meters
Aluminum Thickness	.0022 meters
Cross Sectional Area of Payload Module ¹⁴	.6003 meters ²
Surface Area of the Half Sphere	1.2006 meters ²

1.2.1.1 Cylinder Model

This model assumed that the heat shield was a cylinder with a top disk of area equal to the cross-sectional area of the payload module and as tall as the height of the payload module. This approach gave the largest area of reflection/absorption since the incoming energy was being absorbed by the top and surrounding face of the cylinder – a bigger area than the payload bucket. Upon further iterations of the steady state case for this model, the steady state temperature became a lower number to that compare of the flat

¹⁴ Payload Module takes into account the shape of the structure in figure 5.

plate analysis (see next section) because in part of the model. These were reasonable results-calculations were done correctly- but it was decided to not use this approach to the analysis, in the hopes of creating a more accurate model-considering a magnitude area closer to the actual payload bucket.

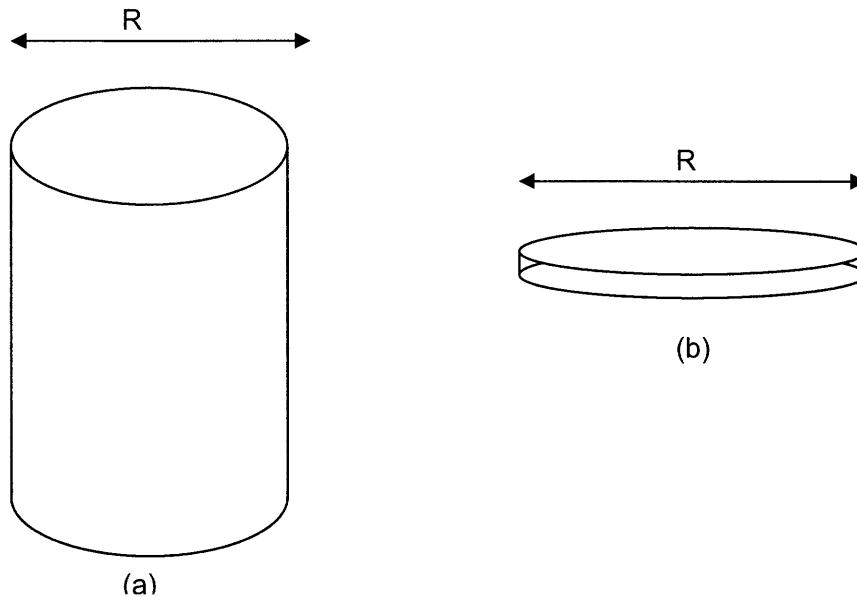


Figure 6. Cylindrical Model (a) versus Flat Plate Model (b). (Same top area for both)

1.2.1.2 Flat Plate Model

Since the top part of the heat shield, which captures most of the incoming external heat flux, can be approximated as a half sphere and the ratio of the radius versus the thickness is significantly larger than 1, the whole structure can be modeled as a flat plate. This model, despite considering the surface area of the plate to be equal to that of the surface area of the half sphere, provides a more accurate analysis. This is true since, the reflective area of the surface is realistically more exact to that of the actual heat shield. For the calculations to be presented the only area not taken into account was the two sides of constant thickness since they are less exposed to the sun (see figure 3).

Furthermore some of the other assumptions taken were: considering the same values for the emissivity on both sides of the heat shield. Mr. Congdon for ARA provided the value of .70 for the absorptivity/emissivity ratio¹⁵. For analysis purposes it was assumed that the absorptivity value was .55 while the emissivity value was .785 since it was not provided by Congdon and they show similar values of other heat shields.

¹⁵ He also provided information on the thermal conductive of the ablator, refer to appendix 4 for these.

Lastly, a zero degree sun incidence angle was used in the calculations to provide for a maximum/worst case scenario.

1.2.2 RESULTS

A steady state analysis was performed as well as a transient analysis. The steady state used a thermal resistances analysis while the transient was modeled as a honeycomb panel with similar thermal properties on both ends as well as a total thermal conductivity equaling that of the Ablator.

1.2.2.1 Steady State

For the steady state case, a thermal circuit conductive analysis was developed and calculated. The $T_{surface}$ K and the T_{inside} refer to the heat shield's outer and inner faces. Figure 4 illustrate the thermal circuit in use.

$$T_{surface} \text{ --- } R_{HeatShield} \text{ --- } T_{inside} \text{ --- } \Sigma R_{MLI \text{ and } Al \text{ sheet}} \text{ --- } T_{bucket}$$

Figure 7. Steady State Thermal Circuit

This steady state analysis takes into account a layer of MLI (Multilayered Insulation) and a layer of Aluminum covering the payload's bucket. The payload bucket is to be maintaining at a temperature of 295.15 ° K (22 ° C). Moreover, the MLI thermal properties were that of Kapton materials which are regularly used for MLI applications.¹⁶

The temperatures at the surface and inside¹⁷ are unknown, though we know the following¹⁸:

¹⁶ Karam's. Thermal Control Hardware Section p. 147.

¹⁷ T_{inside} corresponds to the inside side of the heat shield.

¹⁸ Values for the variables and more calculations are found on the Appendices 1 & 2

$$Q_{absorbed} = Q_{radiated} + Q_{conducted} \quad [0.01]$$

$$Q_{absorbed} = G_s \alpha A_{cross\ section} \quad [0.02]$$

$$Q_{radiated} = \epsilon \sigma A_{surface} T_{surface}^4 \quad [0.03]$$

$$Q_{conducted} = (T_{surface} - T_{inside}) \frac{k * A_{surface}}{L} \quad [0.04]$$

Therefore we can set the following equation and iterate for the value of the $T_{surface}$.

$$Q_{conducted} = G_s \alpha A_{cross\ section} - \epsilon \sigma A_{surface} T_{surface}^4 = \frac{T_{surface} - T_{bucket}}{\Sigma R_{Effective}} \quad [0.05]$$

This iteration leads to $T_{surface}$ value of 305.5 K and a T_{inside} value of 303.7 K.

The following table illustrates the values obtained for the different heat energy interaction from the steady state heat-up period results.

Table 5. Steady State Heat Up Period Results

Energy Process	Heat Energy [Watts]
Energy Absorbed	468.1740
Energy Radiated	466.0843
Energy Conducted	2.097

From the energy conducted we get a heat flux across the heat shield of 3.48 W/m² when you divide the energy conducted by the cross sectional area.

Using the same procedures for the cool down period, this time considering the Earth IR as the absorbed incoming energy instead of the sun, the iteration $T_{surface}$ was 229.95 K while the T_{inside} came out to be 240.13 K. The heat energy values for this period then became:

Table 6. Steady State Cool Down Period Results

Energy Process	Heat Energy [Watts]
Energy Absorbed	137.1371
Energy Radiated	124.4476
Energy Conducted	12.6896

This energy is being conducted outwards since the inside of the heat shield is warmer than the outside. The value for this heat flux is 21.14 W/m^2 .

1.2.2.2 Transient

For the transient analysis, a similar approach to that of a honeycomb as analyzed in Karam's *Satellite Thermal Control for Systems Engineers*¹⁹ was considered. This honeycomb structure, seen as a two node panel, is shown in figure 5.

¹⁹ Satellite's Thermal Analysis, section V, pp 123-145.

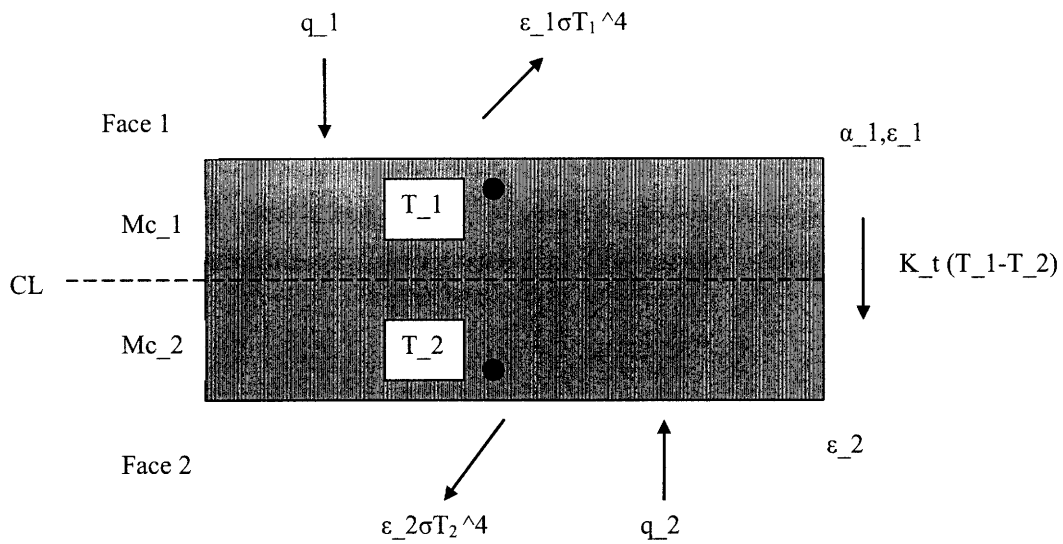


Figure 8. Two Node Panel Model

This approach used a series of equations²⁰ to simplify the calculations, which were used to generate Matlab codes. The results of these programs are presented below.

A. 1st Orbit Heat Up

By taking the linearized equations²¹ for the two sides of figure 5 and plotting the solution to this system, the following graphs were obtained.

²⁰ Refer to Appendix A section V

²¹ Refer to Appendix A section V

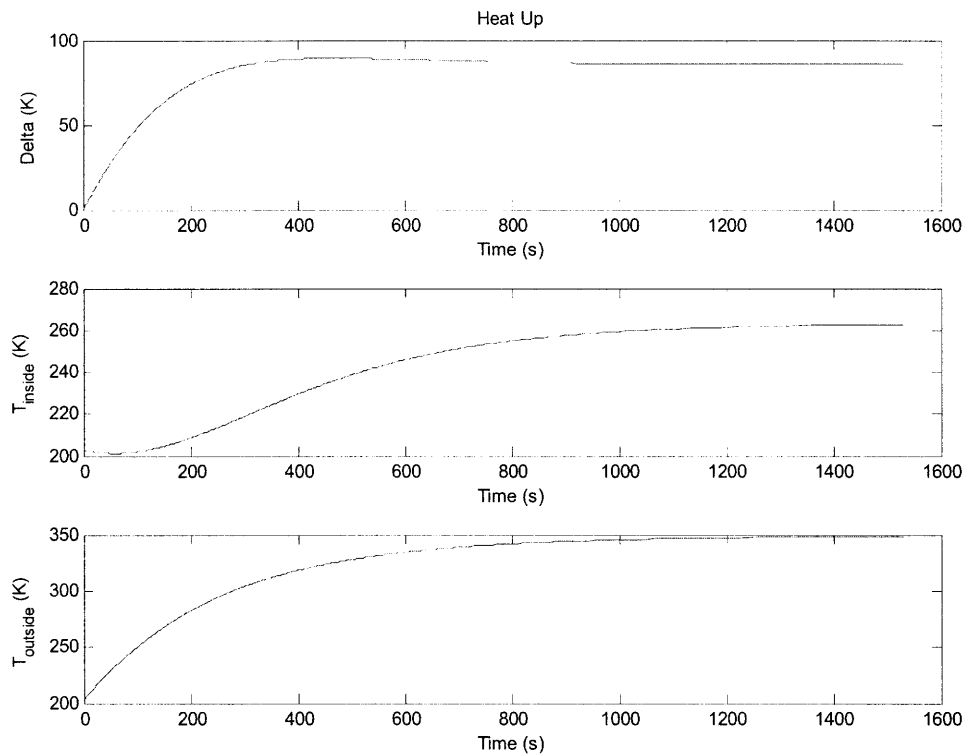


Figure 9. Heat Up 1st Orbit

These results are calculated from an initial temperature of 203 K for the outside of the heat shield. This initial temperature was an assumed temperature for the satellite coming out of the shade²².

For this heat up period, steady state is reached in about 15 minutes²³ while showing a T_{surface} of around 346.5 K and a T_{inside} of 262.5 K.

B. 2nd Orbit Heat Up

Using the T_{surface} from the steady state heat up iteration, 229.95 K, as the initial temperature for the cool down analysis the following result was obtained.

²² This temperature value is the one used in Karam's example. See footnote 19.

²³ On average the satellite will spent about 2300 seconds (~40 minutes) in the shade per orbit.

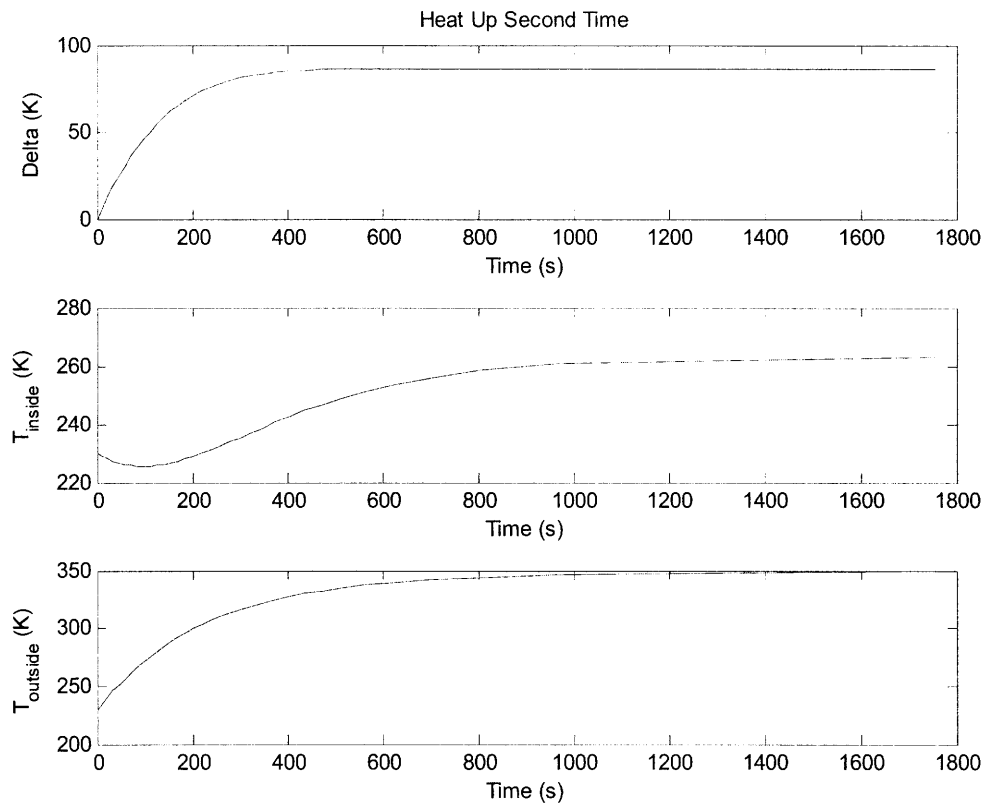


Figure 10. Heat Up 2nd Orbit

The outside surface temperature reaches steady state a little faster than on the previous results but it tends to the same temperature value around 350 K.

This is very reasonable since once at a higher temperature it takes less to heat up.

If we consider the T_{surface} from the transient analysis and plugged it back to the original thermal circuit model we get a heat flux conduction transfer of 15.60 W/m^2 . This is obtained by solving equation 0.04 from a previous section.

1.2.3 CONCLUSION

From my analysis, there will be a small amount of heat going through the heat shield. It should be clear that this analysis was preliminary, thus further conclusions should not be reached solely on the result of these calculations. Regardless, this analysis served to illustrate the current doubts about the heat shield performance and capability of providing the mice in the payload with a suitable living environment.

Note that the difference in steady state temperatures obtained from the Steady State analysis and the Transient analysis is due to the approach for each particular case (honeycomb for the steady state and flat plate for the transient). Though in reality both analysis should reach similar results.

In the Steady State calculations, the analysis considers the MLI and the Aluminum sheet covering the payload bucket as well as the temperature inside the payload bucket. However, the Transient method only accounts for the actual shield and its thermal properties. It should be mentioned that the Transient result is a general solution to the linearized equations, thus it is an approximation and the values for the temperatures can be slightly different to the actual values.

The analysis displays the difference in the heating and cooling down periods as well as the magnitudes and direction of the heat fluxes. Most of the concern should be focus during the sun incidence period since it is here where the analysis shows a heat flux going across heat shield.

To cover concerns related to the *Ginger Snaps*²⁴ initiative, the different values in absorptivities from the different paints can provide significant changes to the performed analysis. This analysis assumed the use of the smallest thickness value for the heat shield, so increasing this thickness and providing greater insulation for the MLI by adding more kapton sheets will take care of the issues established by the variances in absorptivities. The results of changes in absorptivities can be easily obtained by iterating for new temperatures with the new absorptivity values and comparing them to the allowable or acceptable ranges of incoming heat fluxes.

²⁴ Ynis.org initiative

2 REFERENCES

AZ Technologies. *Materials and Coatings Catalog*.
<http://www.aztechnology.com/materials.html>

Goddard Space Flight Center. *Qualified Parts List Directory*.
http://eed.gsfc.nasa.gov/562/qpld/qpld_061704.doc

Honeywell. *Thermal Switches*.
<http://www.honeywell.com/sites/portal?smap=aerospace&page=Thermal-Products3&theme=T4&catID=CBD2344A1-8038-86AA-D33D-39B5B0847DE2&id=HE8D51E65-501F-40EB-2FA1-991BF8C89783&sel=5>

Karam, R.D. "Satellite Thermal Control for Systems Engineers". Progress in Astronautics and Aeronautics. Vol 181. 1998.

Landis, G. Professor at the Aero-Astro Department. Massachusetts Institute of Technology.

Larson W.J., Wertz J.R. "*SPACE MISSION ANALYSIS AND DESIGN*".
Spacecrafts Subsystems: Thermal. 11.5 Third Edition 1999.

MINCO. *Kapton Heaters*. <http://www.minco.com/products/heaters.aspx?id=71>

NANMAC. *Thermocouples*.
<http://nanmac.com/handbook/imagebank.htm>

OMEGA. *Temperature Sensors*.
<http://www.omega.com/techref/measureguide.html>

3 APPENDIX A: EQUATIONS AND METHODS

I. External Input on Top and Bottom Panels

Parameters and Equations

$\alpha = .17$ - Absorptivity of Z-93 Paint

$A_{Bottom} = 1.08 m^2$ - Area of Bottom Face

$A_{Top} = .1526 m^2$ - Area of Top Face

$\epsilon = .92$ - Emissivity of Z-93 Paint

$G_S = 1418 W/m^2$ - Solar Flux Average around Earth

$q_I = 258 W/m^2$ - Max Energy Flux at Earth's Surface

$R_e = 6378.135 * 10^3 m$ - Equatorial Radius of the Earth

$J = 400 * 10^3 m$ - Altitude Above Earth Radius

$\rho = \arcsin \frac{R_e}{J + R_e}$ - For Albedo Effect factor calculations

$K_a = .664 + .521 \rho - .203 \rho^2$ - Albedo Effect Factor

$a = .35$ - Highest Percentage of direct solar energy reflected off the Earth

$G_I = q_I \sin^2(\rho)$ - Energy Flux at Satellite's Location

Incoming Sun

$$Q_{SUN} = G_S * A_{Top} * \alpha$$

Incoming Earth IR

$$Q_{EIR}^{Top} = G_I * A_{Top} * \alpha$$

$$Q_{EIR}^{Bottom} = G_I * A_{Bottom} * \alpha$$

Incoming Albedo to the Bottom Face

$$Q_{Albedo} = G_S * A_{Bottom} * a * \alpha * K_a * \sin^2(\rho)$$

II. External Input on side Panels

Parameters and Equations

$\alpha = .17$ - Absorptivity of Z-93 Paint

$A = 1.5438 \text{ m}^2$ - Total Area of 8 side panels

$\epsilon = .92$ - Emissivity of Z-93 Paint

$G_s = 1418 \text{ W/m}^2$ - Solar Flux Average around Earth

$q_I = 258 \text{ W/m}^2$ - Max Energy Flux at Earth's Surface

$R_e = 6378.135 * 10^3 \text{ m}$ - Equatorial Radius of the Earth

$J = 400 * 10^3 \text{ m}$ - Altitude Above Earth Radius

$\rho = \arcsin \frac{R_e}{J + R_e}$ - For Albedo Effect factor calculations

$K_a = .664 + .521 \rho - .203 \rho^2$ - Albedo Effect Factor

$a = .35$ - Highest Percentage of direct solar energy reflected off the Earth

$G_I = q_I \sin^2(\rho)$ - Energy Flux at Satellite's Location

$\phi = [0 : 2\pi]$ - Angle for Earth IR Calculations

$\phi_2 = [\pi : 2\pi]$ - Angle for Albedo Effects Calculations

Incoming Earth IR to Side Panels

$$Q_{EIR} = G_I * A * \alpha * \cos(\phi)$$

Incoming Albedo to Side Panels

$$Q_{Albedo} = G_s * A * a * \alpha \cos(\phi_2) * K_a * \sin^2(\rho)$$

III. Radiator Area Calculations

In general,

$$A_{radiator} = \frac{Q_{total}}{\epsilon \sigma T^4 - \alpha (q_{sun} + q_{albedo}) + \epsilon q_{Earth}}$$

where,

$$Q_{total} = Q_{top} + Q_{bottom} + Q_{payload} + Q_{electronics}$$

For the case of the Side panels,

$$A_{radiator} = \frac{Q_{total}}{\epsilon \sigma T^4}$$

IV. BUS/RV Separation System

For Lightband:

Outer Radius = .381 m

Inner Radius = .3365 m

$$\text{Area} = \pi (r_{outer}^2 - r_{inner}^2) = .01003 m^2$$

Thickness $t = .1072 m$

Aluminum 7075-T6 Thermal Conductivity $k = 130 W/(m \cdot K)$

Heat Transfer from the Payload to the BUS Through the Lightband

$$Q_{across} = \frac{kA}{t} (T_{payload} - T_{bus})$$

We know that:

$$Q_{across} = 70 W$$

$$T_{payload} = 288.15 K (15 C)$$

Thus, solving for T_{bus} :

$$T_{bus} = 287.547 K (14.424 C)$$

V. Heat Shield Analysis

Constants

$$G_s = 1418 \text{ W/m}^2 \text{ -Solar Flux Average around Earth}$$

$$q_I = 258 \text{ W/m}^2 \text{ -Max Energy Flux at Earth's Surface}$$

$$R_e = 6378.135 * 10^3 \text{ m -Equatorial Radius of the Earth}$$

$$\sigma = 5.67 * 10^{-8} \text{ W/(m}^2 \text{K}^4) \text{ -Stefan-Boltzmann's Constant}$$

Variables

$$\alpha = .55 \text{ -Absorptivity of Ablator}$$

$$A_c = .6002 \text{ m}^2 \text{ -Cross Sectional Area of a Sphere } (\pi r^2)$$

$$A_s = 1.2004 \text{ m}^2 \text{ -Surface Area of a half of a Sphere } (2\pi r^2)$$

$$c = 695.599 \text{ J/(kg K) -Specific Heat of Ablator}$$

$$d = .007 \text{ m -Thickness of Heat Shield}$$

$$\epsilon = .785 \text{ -Emissivity of Ablator}$$

$$\mathfrak{F} = .7 - \left(\frac{\alpha}{\epsilon}\right) \text{ Factor}$$

$$H = 400 * 10^3 \text{ m -Altitude above earth radius}$$

$$k_{hs} = .0014 \text{ W/m} * \text{K -Thermal Conductivity of SD-RAM 20 Ablator/Heat Shield}$$

$$k_{mli} = .0204 \text{ W/m} * \text{K -Thermal Conductivity of Multi Layer Insulation based of Kapton properties}$$

$$k_{al} = 130 \text{ W/m} * \text{K -Thermal Conductivity of Aluminum}$$

$$L_{al} = .0022 \text{ m -Thickness of Aluminum layer}$$

$$L_{hs} = .007 \text{ m -Thickness of Heat Shield layer}$$

$$L_{mli} = .055 \text{ m -Thickness of Multi Layer Insulation layer}$$

$$M = 13.53 \text{ kg -Mass of heat shield}$$

$$\theta = 0 \text{ -Incidence Angle of Sun}$$

$$r = .4371 \text{ m}^2 \text{ -Radius of Sphere}$$

$$T_{bucket} = 295.15 \text{ K -Temperature inside Payload's Bucket}$$

Steady State Analysis

Assuming Constant Incoming Solar Heat Flux

$$Q_{absorbed} = Q_{radiated} + Q_{conducted} \quad [0.01]$$

$$Q_{absorbed} = G_s \alpha A_{cross\ section} \quad [0.02]$$

$$Q_{radiated} = \epsilon \sigma A_{surface} T_{surface}^4 \quad [0.03]$$

$$Q_{conducted} = (T_{surface} - T_{inside}) \frac{k * A_{surface}}{L} \quad [0.04]$$

Thermal Circuit with Heat Flux going through equal to $q = q_{absorbed}$

where $q_{absorbed} = \frac{Q_{absorbed}}{A_{cross\ section}}$ (Heat Flux)

$$T_{surface} \text{ --- } R_{Heat\ Shield} \text{ --- } T_{inside} \text{ --- } \Sigma R_{MLI\ and\ Al\ sheet} \text{ --- } T_{bucket}$$

$$Q_{conducted} = G_s \alpha A_{cross\ section} - \epsilon \sigma A_{surface} T_{surface}^4 = \frac{T_{surface} - T_{bucket}}{\Sigma R_{Effective}} \quad [0.05]$$

$$\Sigma R_{Effective} = R_{MLI} + R_{AL} + R_{HS} \quad [0.06]$$

where,

$$R_{MLI} = \frac{L_{MLI}}{K_{MLI} A_C} \quad R_{AL} = \frac{L_{AL}}{K_{AL} A_C} \quad R_{HS} = \frac{L_{HS}}{K_{HS} A_C} \quad [0.07-0.09]$$

Knowing the Thermal Properties and dimensions for each resistive material and $T_{bucket} = 295.15^\circ K (22^\circ C)$

After a simple iteration procedure, a value of $305.5^\circ K$ is obtained for $T_{surface}$

Single Node Transient Equation

$$Mc \frac{dT}{dt} = Q - KT - A^r \mathfrak{I} \sigma T^4 \quad [1.01]$$

$$T(0^{\text{positive}}) = T_0 \quad [1.02]$$

Dimensionless Form Parameters

$$\tau \equiv \frac{T}{T_0} \quad \theta \equiv \frac{\mathfrak{I} A^r \sigma T_0^3}{Mc} \quad \eta^4 \equiv \frac{Q}{A^r \mathfrak{I} \sigma T_0^4} \quad [1.03-1.05]$$

$$\frac{d\tau}{d\theta} = \eta^4 - \tau^4 \quad [1.06]$$

$$\tau(0^{\text{+}}) = 1.0 \quad [1.07]$$

$$4\eta^3 \theta = \ln \left| \frac{(\eta + \tau)(\eta - 1)}{(\eta - \tau)(\eta + 1)} \right| + 2 \left[\arctan \left(\frac{\tau}{\eta} \right) - \arctan \left(\frac{1}{\eta} \right) \right] \quad [1.08]$$

Satisfies the Final Steady – State Condition: $\tau_{ss} = \eta$

$$T_{ss} = T_0 \left[\frac{Q}{A^r \mathfrak{I} \sigma T_0^4} \right]^{1/4} = \left[\frac{Q}{A^r \mathfrak{I} \sigma} \right]^{1/4} \quad [1.09]$$

HEAT UP OF TWO NODE PANEL

Nonsteady Energy Balance Equations

$$\left(\frac{Mc}{A}\right)_1 \left(\frac{dT_1}{dt}\right) = q_1 - \epsilon_1 \sigma T_1^4 - K_t(T_1 - T_2) \quad [1.10]$$

$$\left(\frac{Mc}{A}\right)_2 \left(\frac{dT_2}{dt}\right) = q_2 - \epsilon_2 \sigma T_2^4 - K_t(T_1 - T_2) \quad [1.11]$$

$$\text{where } T_1 \equiv T_{01}, \quad T_2 \equiv T_{02} \quad [1.12]$$

on Linearization,

$$\left(\frac{Mc}{A}\right)_1 \left(\frac{dT_1}{dt}\right) = q_1 + 3\epsilon_1 \sigma T_m^4 - (4\epsilon_1 T_m^3 + K_t)T_1 + K_t T_2 \quad [1.13]$$

$$\left(\frac{Mc}{A}\right)_2 \left(\frac{dT_2}{dt}\right) = q_2 + 3\epsilon_2 \sigma T_m^4 - (4\epsilon_2 T_m^3 + K_t)T_2 + K_t T_1 \quad [1.14]$$

$$T_1 \equiv T_{01}, \quad T_2 \equiv T_{02}$$

Time derivative of either linear equation

$$\frac{d^2 T_{1,2}}{dt^2} + P \frac{dT_{1,2}}{dt} + Q T_{1,2} = R_{1,2} \quad [1.15]$$

$$P = \left[\frac{A}{Mc}\right] [2K_t + 4(\epsilon_1 + \epsilon_2)\sigma T_m^3] \quad [1.16]$$

$$Q = \left[\frac{A}{Mc}\right]^2 [4(\epsilon_1 + \epsilon_2)K_t \sigma T_m^3 + 16\epsilon_1 \epsilon_2 \sigma T_m^3] \quad [1.17]$$

The subscript 1,2 stands for each node

$$R_{1,2} = \left(\frac{A}{Mc}\right)^2 \left[[K_t(q_1 + q_2) + 3(\epsilon_1 + \epsilon_2)\sigma T_m^4] + 4(q_{1,2} + 3\epsilon_{1,2}\sigma T_m^3)\epsilon_{1,2}\sigma T_m^3 \right] \quad [1.18]$$

The temperature difference $\Delta = T_1 - T_2$ is obtained as

$$\frac{d^2 \Delta}{dt^2} + P \frac{d \Delta}{dt} + Q \Delta = \frac{4(q_1 \epsilon_2 - q_2 \epsilon_1) \sigma T_m^3}{\left(\frac{Mc}{A}\right)^2} \quad [1.19]$$

$$\text{with } \Delta(0) \equiv \Delta_0 \quad [1.20]$$

General Solution for the case when the coefficients are constant is

$$\Delta = C_1 e^{m t} + C_2 e^{n t} + D \quad [1.21]$$

where D ,

$$D = \frac{q_1 \epsilon_2 - q_2 \epsilon_1}{(\epsilon_1 + \epsilon_2) K_t + 4 \epsilon_1 \epsilon_2 \sigma T_m^3} \quad [1.22]$$

where the roots m, n are taken from:

$$p^2 + Pp + Q = 0 \quad [1.23]$$

$$m, n = .5[-P \pm (P^2 - 4Q)^{.5}] \quad [1.24]$$

C_1 and C_2 are determined from the initial conditions:

$$C_1 = \frac{na - b}{n - m} \quad [1.25]$$

$$C_2 = \frac{b - ma}{n - m} \quad [1.26]$$

$$\text{where } a = \Delta_0 - D \quad [1.27]$$

and,

$$b = \frac{(q_1 - q_2) + 3 \sigma T_m^4 (\epsilon_2 - \epsilon_1) - 4 \sigma T_m^3 (\epsilon_1 T_{01} - \epsilon_2 T_{02}) - 2K_t \Delta_0}{\frac{Mc}{A}} \quad [1.28]$$

SRAM-20 Ablator Properties

SRAM-20 ABLATOR THERMAL PROPERTIES

Ablator Density – 20.0 lb/ft³

Temperature Point	Thermal Conductivity, Btu/ft-sec-°R	Heat Capacity, Btu/lb-°R	Absorptivity/Emissivity
250	0.0000050	0.205	0.70
310	0.0000057	0.205	0.70
460	0.0000077	0.262	0.70
510	0.0000079	0.277	0.70
560	0.0000090	0.285	0.70
750	0.0000115	0.288	0.70

4 APPENDIX B: GRAPHS , DATA OBTAINED and CAD MODELS

The data provided in the following graphs and tables were calculated from the Equations in Appendix A.

Figure 11. Side Panels Incoming Heat

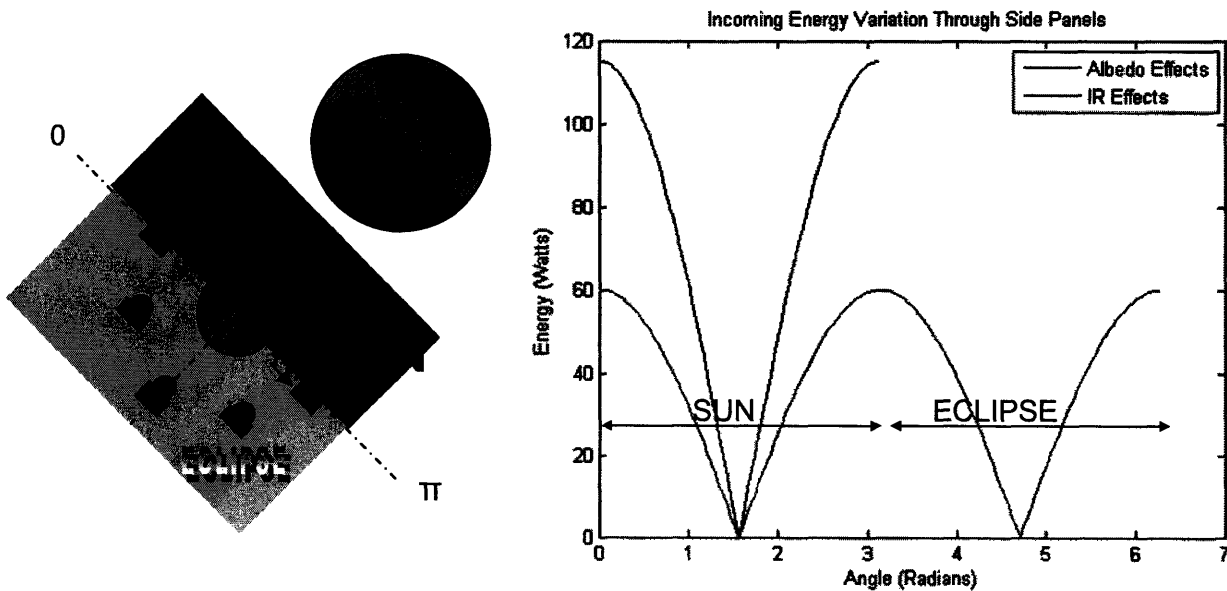
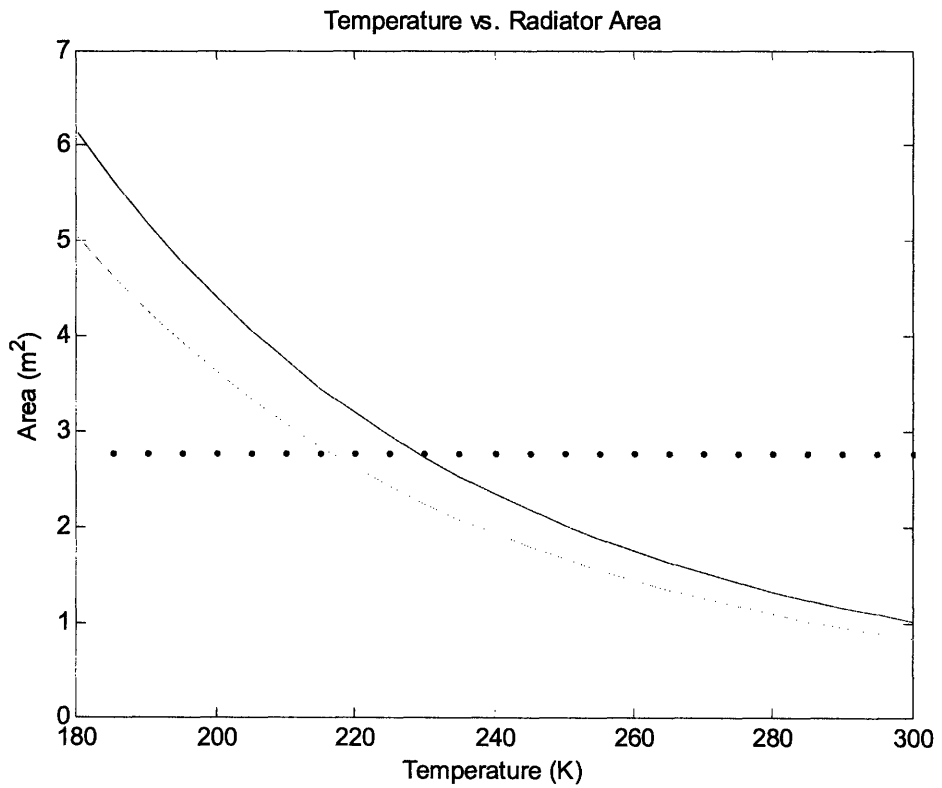


Table 7. External Heat Input Comparison

SOURCE	BUS (Top/Bottom)		BUS Side Panels	
	SUN	X	TOP	X
Albedo	X	BOTTOM	X	YES
Earth IR	TOP	BOTTOM	YES	YES

SOURCE	BUS (Top/Bottom)		BUS Side Panels	
	SUN	X	36.79 W	X
Albedo	X	80.50 W	X	115 W (MAX)
Earth IR	32.07 W	41.94 W	60 W (MAX)	60 W (MAX)

Figure 12. Temperature versus radiator area



Optimal Value at 236 K for an estimated 450 W of heat being dissipated.
 If the heat dissipated were about 370 W, the optimal value is at 217 K. (Green Line)
 Red Line indicates Max Radiator Area Available.

CAD MODELS DRAWINGS

Figure 13. Bus Dimension in millimeters

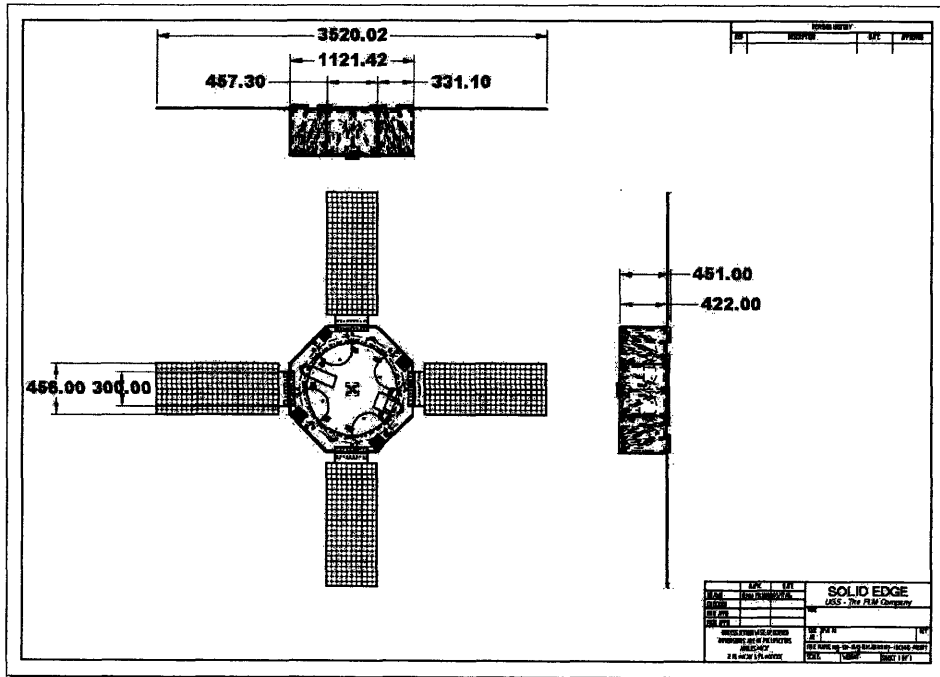


Figure 14. Payload/Heat Shield Dimensions in centimeters

